Volume 24, No 3 | International Journal of Radiation Research, July 2026

A Simulation and experimental study on neutron attenuation of polyester composites incorporated with boron carbide micro- and nano-particles

S. Sabokro[1], J. Moradgholi[2], P. Rafiepour[3], S.M.J. Mortazavi[1,4*]

[1]Medical Physics and Engineering Department, School of Medicine, Shiraz University of Medical Sciences, Shiraz, Iran
[2]Department of Materials Engineering, Isfahan University of Technology (IUT), Isfahan, Iran
[3]School of Engineering, Persian Gulf University, Mahini Ave, Bushehr 7516913817, Iran
[4]Ionizing and Non-ionizing Radiation Protection Research Center (INIRPRC), Shiraz University of Medical Sciences, Shiraz, Iran

► ***Original article***

Corresponding author:
S. Mohamad J. Mortazavi, Ph.D.,
E-mail: *mortazavismj@gmail.com*

Received: September 2025
Final revised: July 2026
Accepted: July 2026

Int. J. Radiat. Res., July 2026; 24(3): 779-787

DOI: 10.61186/ijrr.24.3.27

Keywords: *Neutrons, polyesters, boron carbide, nanoparticles, microparticles*

ABSTRACT

Background: To mitigate neutron exposure hazards in industries like aerospace, flexible, lightweight polymer-based shields with high-temperature tolerance have been developed using suitable fillers that moderate fast neutrons and capture slow neutrons, ensuring reliable radiation protection. ***Material and Methods:*** This study involved exposing unsaturated polyester resin (UPS) composites reinforced with nano- and micro-sized boron carbide (B_4C) to neutron radiation from a ^{239}Pu–Be source. Various weight percentages (0.5%, 1%, 2%, and 5%) of nano- and micro-B_4C fillers, along with thicknesses of 2.5 mm, 5 mm, 7.5 mm, and 10 mm, were evaluated. Experimental measurements were carried out to count fast and thermal neutrons, measure the macroscopic cross-section, half value layer, and Geant4 Monte Carlo simulations were performed for benchmarking. ***Results:*** Higher concentrations of B_4C resulted in increased total cross-section values and decreased half-value thickness measurements. At 5mm, 7.5mm, and 10 mm thicknesses, significant differences between nano- and micro-composites emerged at 2 wt.% ($p < 0.05$), becoming more pronounced with higher filler concentrations and greater sample thickness. These findings confirm the superior neutron attenuation performance of nano-sized B_4C, attributed to its higher surface-to-volume ratio and improved dispersion within the matrix. Geant4 simulations closely matched the experimental data at higher filler loadings, except under certain conditions. ***Conclusion:*** Both experimental and simulation results confirmed that protection improves with increased thickness and filler weight percentages, as expected. The study also highlighted the impact of nanotechnology on shielding properties, showing its advantage over micro-sized samples.

INTRODUCTION

Exposure to neutrons poses a significant hazard to human health due to their higher linear energy transfer (LET) compared to electrons and photons. Neutrons can cause severe, often irreparable damage to human organs and operational disruptions to space electronics, necessitating enhanced protection in aerospace, medical, and industrial applications [1, 2]. Exposure to neutron radiation has been linked to neurological disorders, vomiting, decreased blood count, nausea, and hematopoietic syndrome in humans [3, 4].

Different types of neutron radiation exist in space, including high-energy (fast), low-energy (thermal, epithermal, or slow), and backscattered neutrons [5]. Different types of neutron radiation exist in space, including high-energy (fast), low-energy (thermal, epithermal, or slow), and backscattered neutrons [6]. Hydrogen nuclei are particularly effective in neutron absorption because their mass closely matches that of neutrons and they do not produce secondary neutrons. Thus, suitable neutron shielding materials should contain a high hydrogen content along with elements possessing a large neutron absorption cross -section [7, 8].

Polyethylene, a hydrogen-rich thermoplastic polymer, is widely used for fast neutron shielding due to its low density and effective protective properties. However, despite its excellent radiation shielding capability, pure polyethylene lacks the necessary thermal stability and structural strength required for protective applications [9]. Consequently, many research groups have focused on developing multipurpose composites that use polyethylene as a base material [10].

More recently, thermoset matrices have been increasingly employed over thermoplastic polymers

in the production of advanced composite materials, owing to their superior cross-linked properties, durability, strength, thermal stability, and chemical resistance [11-13]. Therefore, there is a lot of interest in using polystyrene instead of polyethylene as a polymer substrate for neutron shielding [14, 15].

To further enhance neutron shielding and overall performance, various additives with high thermal neutron cross-sections - such as boron (^{10}B) [16-18], lithium (^{6}Li) [19, 20], and cadmium (^{113}Cd) [21, 22] - can be incorporated into the polymer matrix. These additives not only improve neutron shielding but also enhance mechanical strength and thermal insulation. Particularly in polyester matrix composites, micro- and nano-fillers can significantly improve the mechanical properties of polymers [23]. The highest thermal neutron absorption cross-section among ^{10}B compounds is 3840 barns (1 barn = 10^{-24} cm^2) [24].

Boron compounds are especially attractive due to their natural abundance, low density, affordability, low-energy secondary photon production, low weight, non-toxic nature, and consistent neutron absorption performance across various energy levels. Their safe composition and ease of manufacturing also make them ideal as fillers in shielding materials [25, 26].

The primary boron-based neutron absorbers include boron carbide (B_4C), boron trioxide (B_2O_3), boron nitride (BN), and boric acid (H_3BO_3) [27-31]. Among these, B_4C exhibits the highest theoretical cross-section for thermal neutron absorption and generates low-energy secondary photons [29, 32]. B_4C is widely utilized in high-performance applications due to its remarkable properties, including extreme hardness, high melting point, low density, and excellent resistance to chemical agents, as well as superior thermoelastic, thermoelectric, corrosion, and oxidation resistance. These features have led to its extensive use in various high-performance fields, including nuclear and aerospace applications [33, 34].

In this study, we investigated a new composite based on unsaturated polyester (UPS) filled with nano- and micro-sized B_4C particles at varying weight percentages (0.5-5 wt.%) and sample thicknesses (2.5-10 mm). This composite avoids the toxicity of cadmium and overcomes the limitations of polyethylene noted previously. This study is the first to develop the neutron shielding efficiency of nano-B_4C fillers and to compare the shielding performance of nano- and micro-sized B_4C within equivalent matrices and experimental environments, supported by statistical analysis. Geant4 Monte Carlo simulation was employed to validate the experimental results. This combined experimental and computational approach represents a significant step toward systematically designing and validating next-generation lightweight, flexible, and highly efficient neutron shielding materials.

MATERIALS AND METHODS

Experimental study

Fabrication of samples: In this study, composites were fabricated using commercially available unsaturated polyester resin (UPS) (Knowledge-Based Companies Campus, Abadeh, Fars, Iran) as the polymer base. The reinforcements and radiation shielding component, B_4C, was supplied by Neutrino Company (Tehran, Iran) in both micro- (~100 μm) and nano-sized (~50 nm) forms. First, the commercial UPS was weighed, and 0.4% cobalt (as an accelerator) (Knowledge-Based Companies Campus, Abadeh, Fars, Iran) was added to prepare the polymer matrix for blending with B_4C filler. Micro-sized B_4C particles were then mixed with the resin at the desired weight percentages (0%, 0.5%, 1%, 2%, and 5%). For the nano-B_4C, 50 nm particles were uniformly dispersed in the polyester matrix using ultrasonic methods to enhance dispersion and consistency.

The prepared solutions were poured into disc-shaped molds with a 4 cm radius and thicknesses of 2.5, 5, and 10 mm. A hardener, 1.38 wt.% methyl ethyl ketone peroxide (Knowledge-Based Companies Campus, Abadeh, Fars, Iran), was added to initiate the curing reaction. The curing process took approximately 12 hours. The composites were then annealed in an oven at 40 °C for one day. Additionally, 2.5 mm and 5 mm samples were stacked to construct the 7.5 mm samples. In total, 36 samples were prepared, including four without filler, 16 with UPS/nano-B_4C, and 16 with UPS/micro-B_4C (figure 1).

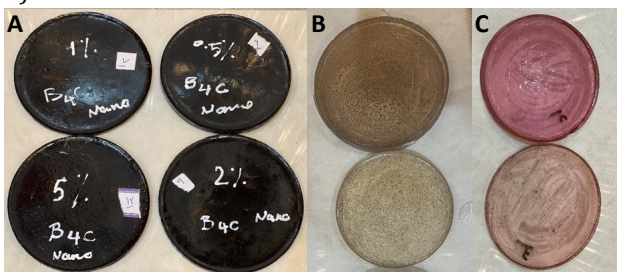

Figure 1. The prepared polyester/boron carbide(B4C) composites with **(a)** nano-B_4C and **(b)** micro-B_4C. **(c)** The control samples (pure polyesters) are shown on the right side.

Theoretical formula: Two mechanisms govern the interaction of neutrons with materials: scattering and absorption. Neutron scattering comprises both elastic and inelastic scattering processes. The absorption process includes nuclear reactions, activation, fission, and related interactions. The probability of the neutron interaction with a target nucleus is expressed with the total microscopic cross-section, σ_{tot} (barns), which is the sum of the absorption (σ_A) and scattering (σ_S) cross-sections. The total macroscopic cross-section, Σ_{tot}, (1/cm) is obtained by equation 1-a [35] or calculated from Beer-Lambert

Law (equation1-b)[36]:

1) a) $\sum_{tot} = \sum_i N_i (\sigma_{tot})_i$ or b) $I = I_0 e^{-\Sigma tot \times x}$

where; N_i is the atom density (i.e., the number of nuclei per unit volume).

The half value layer (HVL) of the composite is calculated by equation 2 [37]:

2) $HVL = \ln 2/\sum \cong 0.693/\sum$

The neutron attenuation can be calculated using equation 3:

3) $\frac{I_0 - I}{I_0} = 1 - e^{-\sum_{tot} \times x}$

Where; x is the sample thickness, and I and I_0 are the neutron flux recorded by the detector with and without the composite, respectively.

Neutron attenuation measurements: The samples were irradiated using a ^{239}Pu–Be neutron source (Radiation Research Center, Shiraz University, Shiraz, Fars, Iran) with an activity of 4.6 Ci (±0.03 Ci). Figure 2 presents a schematic of the neutron source and detector setup. Polymeric granules, serving as the moderator material, were placed inside a cylindrical holder alongside the neutron source. A neutron meter (Model 488A) (Radiation Research Center, Shiraz University, Shiraz, Fars, Iran) equipped with a boron probe with a radius of 1.3 cm was used as the neutron detector. The distance between the detector and the ^{239}Pu–Be source was maintained at 5.5 cm.

To detect both fast and thermal neutrons (total neutrons), a polyethylene casing was applied around the boron probe. Polyethylene was selected for its effective moderation of emitted neutrons, bringing them into the thermal energy range and enhancing the probability of absorption by the target nucleus [22]. This method replaces a solid moderator, like polyethylene blocks, with a non-static medium such as water, to slow down neutrons [38]. Consequently, the polyethylene coating converts fast neutrons into thermal neutrons, enabling the measurement of both types. The I value was calculated at various micro- and nano-B_4C concentrations using Equation 3. Each experiment was conducted in triplicate.

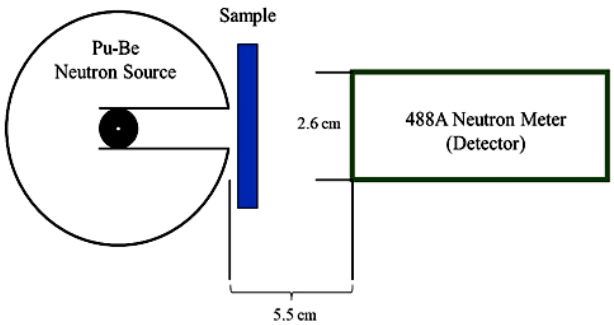

Figure 2. An illustration of the neutron source, sample, and detector.

Simulation study

Monte Carlo Simulation toolkit: The simulation component of this study was performed using the Geant4 (version 11.0) Monte Carlo toolkit [39]. Geant4, developed in C++, is a versatile and widely validated simulation platform used extensively in ionizing radiation shielding studies [40-43]. The QGSP_BIC_HP physics list was employed to define the physical interactions with matter, including hadronic (elastic and inelastic), decay, standard electromagnetic, and high-precision neutron physics models - suitable for radiation protection and dosimetry applications [44, 45]. Simulations were executed on a computing system featuring a 60-core CPU and 160 GB of RAM.

Geometry and source definition: B_4C micro- and nano-particles were modeled as simple spheres embedded in a polymer cube, representing the composite matrix (figure 3a). The radius of the sphere and the side length of the cube were adjusted to achieve the desired filler concentration, defined using equation 4:

$$\text{Concentration (wt.\%)} = 100 \times (\rho_f \times V_f)/(\rho_m \times V_m) \quad (4)$$

Where; ρ and V represent the density and volume of the filler and matrix, respectively. By increasing the sphere radius relative to the cube side length, filler concentration increased, and vice versa. The cube was then replicated in a 3D grid to model a complete sample consistent with the actual experimental thicknesses. Figure 3b shows the lattice structure of a small cube of polyester with a side length of 1 mm and a filler concentration of 5%.

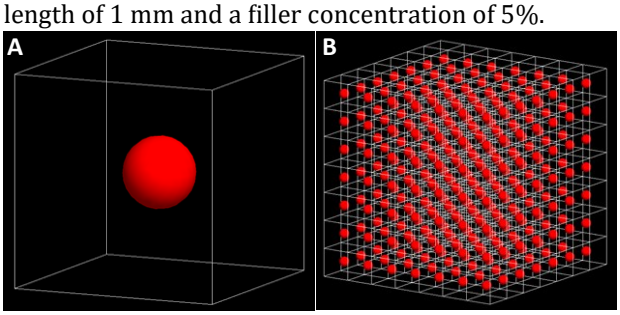

Figure 3. An illustration of boron carbide (B_4C) filler (red sphere) inside the polyester substrate **(a)**. The lattice structure of the sample simulated as a small cube with a side of 1 mm and a filler concentration of 5% **(b)**.

The radiation source was simulated in two stages. First, a ^{239}Pu–Be neutron source was modeled in a vacuum, and the energy spectrum of emitted neutrons was recorded in a phase space file. In the second stage, the source was defined as a pure neutron emitter using this recorded spectrum. Figure 4 illustrates the collimated neutron transport towards the sample.

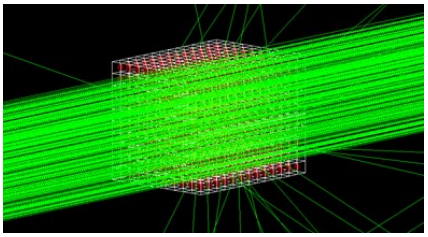

Figure 4. A view of the transport of collimated neutrons towards the sample.

Since only neutron counts entering the detector were required, the detector material was defined as air in the simulation. While the detector type affects volume flux calculations, in this study the surface flux was calculated at the detector face. Neutrons arriving at the detector surface were recorded with and without the composite samples, and neutron attenuation was calculated using equation 3. From the sample thickness and this attenuation, the macroscopic neutron cross-section was determined. Simulations employed 8×10^8 primary neutrons, resulting in a statistical uncertainty below 1%.

RESULTS

Experimental findings

Total neutron rate: Figures 5(a) - 5(d) show the mean total neutron rate (thermal and fast) in counts per minute for composite samples with thicknesses of 2.5, 5, 7.5, and 10 mm, respectively. Neutron counts were measured for each weight percentage (wt.%) of the B_4C nano- and micro-fillers. Mean and standard deviation were reported to represent the total neutron rate. The mean total neutron flux without any sample present was 653±31 counts/min. Independent t-tests were used to assess differences between samples with nano- and micro-fillers at each thickness and filler concentration. Statistical significance was defined as $p<0.05$. The mean total neutron rates (counts/min), total macroscopic cross-sections (cm^{-1}±SD), and corresponding p-values are summarized in table 1. Additionally, the corresponding half-value layers (HVLs, in cm±SD) and their p-values are presented in table 2. Error bars in figure 5 represent 10% of the data.

Table 1. Total Neutron Rate (Count/min) reached the detector and the total macroscopic cross-section of neutrons (fast and thermal) for nano- and micro-boron carbide (B_4C) in polyester composite with 2.5mm, 5mm, 7.5mm, and 10 mm thicknesses as well as different weight percentages (wt.%) of the filler (0.0%, 0.5%, 1%, 2%, 5% of B_4C).

Thickness (mm)	Wt.%	I (Count/min)(Mean ± SD)		*p*-value
		Nano filler	Micro filler	
2.5	% 0.5	45 ± 628	44 ± 628	1.00
	% 1.0	43 ± 617	42 ± 623	0.35
	% 2.0	41 ± 607	43 ± 619	0.21
	% 5.0	39 ± 586	41 ± 614	0.12
5.0	% 0.5	43 ± 602	44 ± 602	1.00
	% 1.0	41 ± 581	42 ± 594	0.28
	% 2.0	37 ± 522	40 ± 554	*0.02
	% 5.0	38 ± 526	42 ± 577	*0.001
7.5	% 0.5	42 ± 578	41 ± 578	1.00
	% 1.0	40 ± 550	41 ± 566	0.18
	% 2.0	37 ± 522	40 ± 554	*0.02
	% 5.0	35 ± 472	39 ± 543	*0.001
10	% 0.5	41 ± 560	40 ± 554	0.76
	% 1.0	39 ± 518	38 ± 540	0.12
	% 2.0	36 ± 484	38 ± 525	*0.01
	% 5.0	33 ± 423	37 ± 510	*0.0005

SD = Standard deviation, Wt.% = weight percentages, I = Total Neutron Rate (Count/min), = Macroscopic cross-section, * P-value <0.05

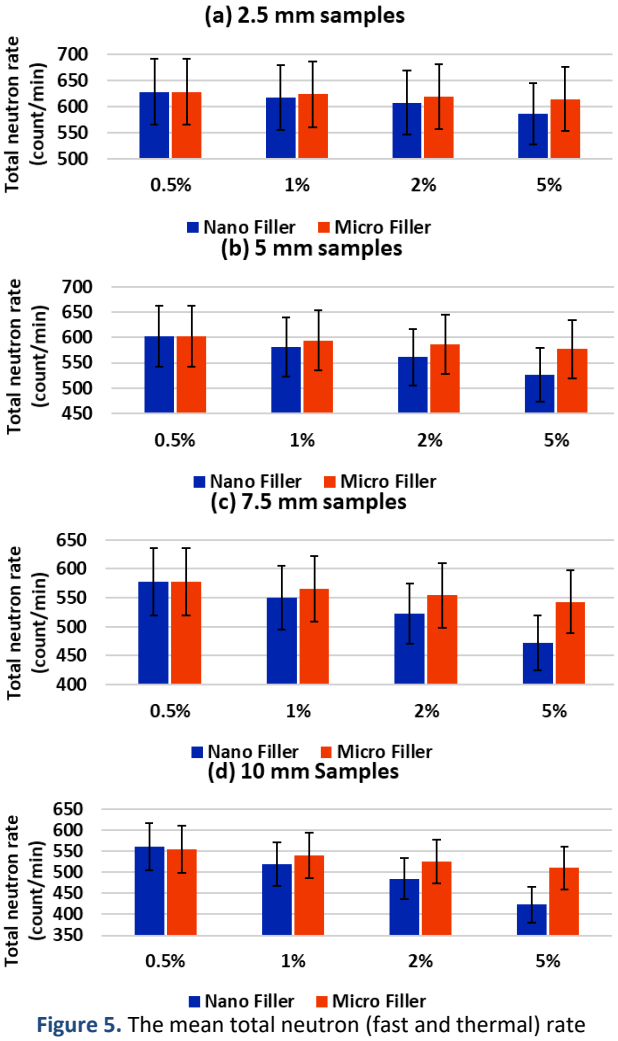

Figure 5. The mean total neutron (fast and thermal) rate (count per min) reached the detector through **(a)** 2.5 mm, **(b)** 5 mm, **(c)** 7.5 mm, and **(d)** 10 mm polyester/boron carbide (B_4C) composites of 0.5, 1, 2, and 5 weight percentages(wt.%) of the nano- and micro-B_4C.

The mean total neutron rates measured for the control samples (UPS without fillers) were 638±45, 624±43, 609±41, and 596±40 count/min for thicknesses of 2.5, 5, 7.5, and 10 mm, respectively. As shown in figure 5 and tables 1, for the 2.5 mm thickness, the mean total neutron rate with 0.5 wt.% of B_4C nano-filler was 628±45 count/min. This rate decreased to 617±43, 607±41, and 586±39 count/min for 1, 2, and 5 wt.% of B_4C nano-filler, respectively. The corresponding rates for B_4C micro-fillers were 628±44, 623±42, 619±43, and 614±41 count/min. At this thickness, no statistically significant differences were observed between nano- and micro-fillers ($p>0.05$). Similarly, at other thicknesses (5, 7.5, and 10 mm) with 0.5 and 1 wt.% of filler, no statistically significant differences were found ($p>0.05$). However, differences became apparent at 2 and 5 wt.% (figure 5 and table 1).

For instance, at 5 mm with 5 wt.% nano-filler, the mean total neutron rate was significantly lower (526 ± 36 counts/min) compared to the micro-filled composites (577±42 counts/min), with a p-value of

0.001. At 7.5 mm (table 1), the neutron rate for the nano-filled sample dropped to 472±35 counts/min, while the micro-filled sample remained higher at 543±39 counts/min (p=0.001). At 10 mm, the mean total neutron rate with 0.5 wt.% B_4C nano-filler was 560±41 counts/min, decreasing to 518 ± 39, 484 ± 36, and 423 ± 33 counts/min at 1, 2, and 5 wt.% loadings, respectively. For the B_4C micro-fillers, the corresponding rates were 554±40, 540±38, 525±38, and 510±37 counts/min (figure 5 and table 1). At this thickness, nano-fillers consistently outperformed micro-fillers, particularly at 5 wt.% loading, where neutron rates were 423±33 counts/min for nano-filled samples compared to 510 ± 37 counts/min for micro-filled samples (p=0.0005), indicating significantly enhanced neutron attenuation with nano -filler formulations.

Figure 6 illustrates the total neutron rates detected in polyester composites containing 5 wt.% nano- and micro-B_4C fillers. Error bars in figure 6 represent 10% of the data.

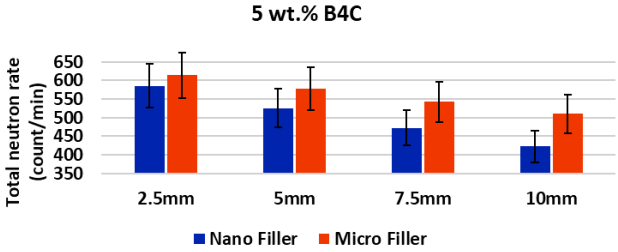

Figure 6. Variations in the total neutrons (fast and thermal) rate (count per min) through polyester/nano- and micro-boron carbide(B_4C) composites at different sample thicknesses (2.5, 5, 7.5, 10 mm) containing 5 weight percentages (wt.%) of nano- and micro-B_4C.

As shown in figure 6 and summarized in table 1, the total neutron rates (fast and thermal) for polyester composites with 5 wt.% nano- and micro-sized B_4C fillers were measured at different thicknesses. Neutron transmission decreased with increasing sample thickness for both filler types, indicating improved shielding. At 2.5 mm, the total neutron rate was 58±39 counts/min for nano-filled samples and 614±41 counts/min for micro-filled samples (p=0.12), showing no significant difference. However, at 5 mm thickness, a statistically significant reduction in neutron rate was observed for nano-filled samples (526±38 vs. 577±42 counts/min, p=0.001). This difference became more pronounced at 7.5 mm (472±35 vs. 543±39 counts/min, p=0.001) and reached a high level of statistical significance at 10 mm (423±33 vs. 510±37 counts/min, p=0.0005). These results demonstrate that nano-sized B_4C fillers provide enhanced neutron attenuation compared to micro-sized fillers, especially at higher sample thicknesses. This is likely due to the improved dispersion and higher surface area of nano-fillers, which facilitate more effective interactions with incoming neutrons.

Macroscopic cross-section (Σ) and half value layer (HVL): The total neutron macroscopic cross-section (Σ) for both nano- and micro-B_4C-filled polyester composites increased with rising B_4C filler concentrations across all thicknesses (2.5 mm to 10 mm), indicating enhanced neutron attenuation. For the control samples, Σ was 0.0934±0.005 cm^{-1}, 0.0929±0.005 cm^{-1}, 0.0928±0.005 cm^{-1}, and 0.0102±0.005 cm^{-1} for thicknesses of 2.5, 5, 7.5, and 10 mm, respectively. From 1.0 wt.% to 5.0 wt.%, the nano-B_4C composites consistently exhibited significantly higher Σ values than their micro counterparts. Differences were especially pronounced at 2.0 wt.% and 5.0 wt.% B_4C. For example, at 2.5 mm thickness and 5.0 wt.% B_4C, Σ was 0.433±0.0001 cm^{-1} for nano-filled composites compared to 0.247 ± 0.0007 cm^{-1} for micro-filled ones (p<0.00001). These trends persisted across all thicknesses, demonstrating nano-B_4C's superior capacity to interact with neutrons. Statistical comparisons showed that below 1.0 wt.% filler content, the difference between nano and micro fillers was not significant (p>0.05). However, as filler content increased, the improvements in Σ for nano composites became statistically significant, with p-values ranging from 0.0011 to <0.00001 (table 2).

Table 2. Neutron macroscopic cross-section (cm^{-1}) for nano- and micro-boron carbide (B_4C) in polyester composite with 2.5mm, 5mm, 7.5mm, and 10 mm thicknesses as well as different weight percentages (wt.%) of the filler (0.0%, 0.5%, 1%, 2%, 5% of B_4C).

Thickness (mm)	Wt.%	Σ (cm^{-1} ± SD)		*p*-value
		Nano filler	Micro filler	
2.5	% 0.5	0.0009±0.157	0.0009 ±0.157	1.00
	% 1.0	0.0012±0.228	0.0009 ±0.189	*0.0011
	% 2.0	0.0009±0.293	0.0012 ±0.215	*0.00006
	% 5.0	0.0001±0.433	0.0007 ±0.247	*0.00001>
5.0	% 0.5	0.0004±0.163	0.0004 ±0.163	1.00
	% 1.0	0.0004±0.234	0.0007 ±0.190	*0.0008
	% 2.0	0.0004±0.304	0.0005 ±0.217	*0.00003
	% 5.0	0.0005±0.432	0.0006 ±0.248	*0.00001>
7.5	% 0.5	0.0008±0.163	0.0008 ±0.163	1.00
	% 1.0	0.0007±0.229	0.0009 ±0.191	*0.0010
	% 2.0	0.0002±0.298	0.0004 ±0.219	*0.00004
	% 5.0	0.0007±0.431	0.0007 ±0.246	*0.00001>
10	% 0.5	0.0004±0.154	0.0006 ±0.165	*0.0260
	% 1.0	0.0006 ±0.231	0.0001 ±0.190	*0.0009
	% 2.0	0.0006 ±0.300	0.0001 ±0.218	*0.00003
	% 5.0	0.0002 ±0.434	0.0001 ±0.247	*0.00001>

SD = Standard deviation, Wt.% = weight percentages, Σ (cm^{-1}) = Macroscopic cross-section, * P-value <0.05

Table 3. The half value layer (HVL) of neutrons for nano- and micro-boron carbide(B_4C) in polyester composite with different weight percentages (wt.%) of the filler (0.0%, 0.5%, 1%, 2%, 5% of B_4C).

Wt.% of B_4C in composite samples	HVL (cm ± SD)		*p*-value
	Nano filler	Micro filler	
% 0.5	0.106 ± 4.36	0.083 ± 4.28	0.363
% 1.0	0.031 ± 3.00	0.027 ± 3.65	*0.0007
% 2.0	0.032 ± 2.32	0.027 ± 3.19	*0.001
% 5.0	0.0043 ± 1.59	0.0043 ± 2.80	*0.00001 >

SD = Standard deviation, Wt.%= weight percentages,* P-value <0.05

As shown in table 3, at 0.5 wt.% filler, the

difference in HVL between nano and micro fillers was not statistically significant (p>0.05). However, at 1.0, 2.0, and 5.0 wt.% B_4C, the differences were highly significant (p<0.001).

Simulation findings

Neutron attenuation, calculated as $(1-(I/I_0))$, was determined for the samples containing polyester with 2 wt.% and 5 wt.% of nano-B_4C filler at thicknesses of 5 mm and 10 mm. Results from Monte Carlo simulations were compared with experimental data (figure 7, table 4). For 2 wt.% nano-B_4C filler at 5 mm thickness, the experimentally derived attenuation was 0.060 ± 0.005, matching the corresponding Geant4 simulation result of 0.060 ± 0.005.

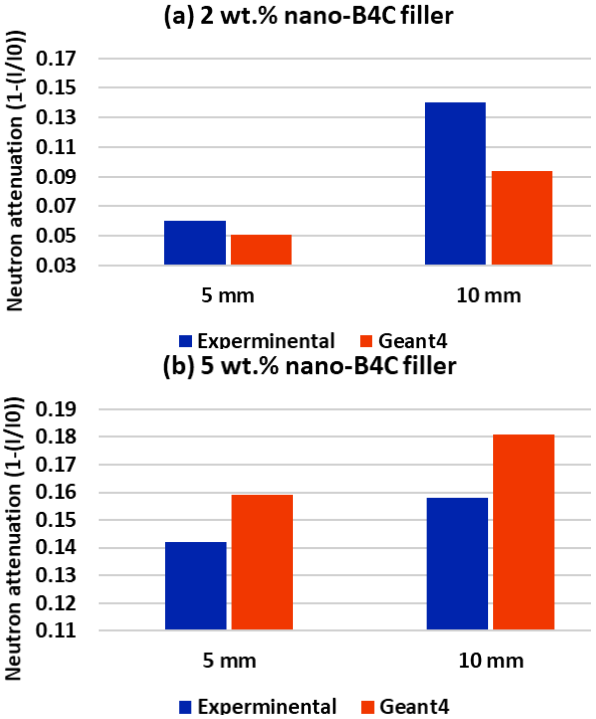

Figure 7. The attenuation of neutrons (fast and thermal) in the composite samples with **(a)** 2 weight percentages (wt.%) and **(b)** 5 wt. % nano-boron carbide (B_4C) fillers for a composite thickness of 5 and 10 mm.

Table 4. The neutron attenuation (1-(I/I0)) of experimental vs. Geant4 simulated values for nano-sized B_4C fillers at **(a)** 2 wt.% and **(b)** 5 wt.%, and sample thicknesses of 5 mm and 10 mm.

A

Thickness (mm)	Method	$1-(I/I_0)$ (Mean ± SD)	*p*-value (Exp vs Geant4)
5	Experimental	0.060±0.005	0.03*
	Geant4	0.051±0.004	
10	Experimental	0.140±0.006	0.001*
	Geant4	0.094±0.005	

B

Thickness (mm)	Method	$1-(I/I_0)$ (Mean ± SD)	*p*-value (Exp vs Geant4)
5	Experimental	0.142±0.006	0.04*
	Geant4	0.159±0.005	
10	Experimental	0.158±0.006	0.01*
	Geant4	0.181±0.006	

I = measured intensity, I0 = baseline intensity, SD = Standard deviation, Wt.%= weight percentages, vs = versus, * P-value <0.05

Figure 8 and table 5 illustrate the neutron attenuation values for samples containing polyester with 1 wt.% and 5 wt.% nano-B_4C filler at both 5 mm and 10 mm thicknesses. At 1 wt.% and 5 mm thickness, the experimental attenuation (0.077±0.004) exceeded the Geant4 simulation (0.060±0.004, p=0.02). At 5 wt.% and 5 mm thickness, however, experimental and simulated results were in close agreement (0.116±0.005 vs. 0.117±0.004, p=0.92). This agreement did not extend to 10 mm thickness, where Geant4 simulations overestimated attenuation (0.240±0.005) compared to the experimental value (0.220±0.006, p=0.01).

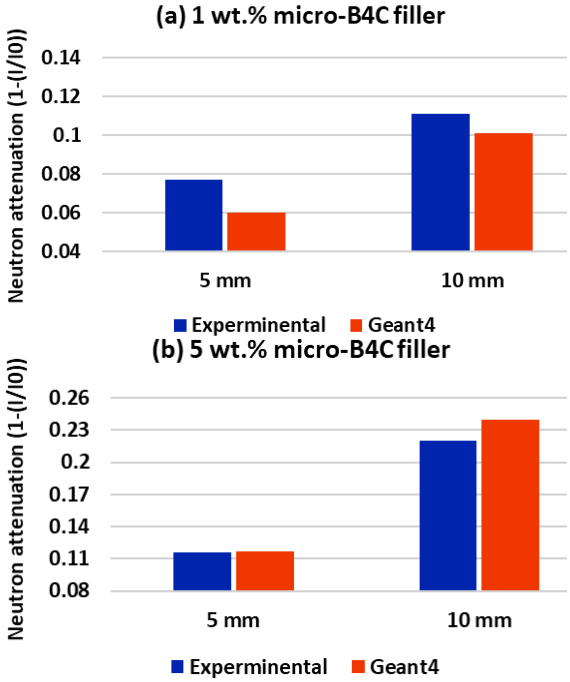

Figure 8. The attenuation of neutrons (fast and thermal) in the composite samples with **(a)** 1 weight percentages (wt.%) and **(b)** 5 wt. % micro- boron carbide (B_4C) fillers for a composite thickness of 5 and 10 mm.

Table 5. The neutron attenuation (1-(I/I0)) of experimental vs. Geant4 simulated values for micro-sized B_4C fillers at **(a)** 1 wt.% and **(b)** 5 wt.%, and sample thicknesses of 5 mm and 10 mm.

A

Thickness (mm)	Method	$1-(I/I_0)$ (Mean ± SD)	*p*-value (Exp vs Geant4)
5	Experimental	0.077±0.004	0.02*
	Geant4	0.060±0.004	
10	Experimental	0.111±0.005	0.04*
	Geant4	0.101±0.004	

B

Thickness (mm)	Method	$1-(I/I_0)$ (Mean ± SD)	*p*-value (Exp vs Geant4)
5	Experimental	0.116±0.005	0.92
	Geant4	0.117±0.004	
10	Experimental	0.220±0.006	0.01*
	Geant4	0.240±0.005	

I = measured intensity, I0 = baseline intensity, SD = Standard deviation, Wt.%= weight percentages,* P-value <0.05

As shown in figures 7 and 8, overall, the simulation results agreed well with the experimental data, except

for the 10 mm thick sample with 5 wt.% nano-B_4C filler. The relative difference for this sample was 32.8%. For micro-B_4C composites, the maximum relative difference was 22% for the 1 wt.% micro-B_4C composite.

DISCUSSION

As shown in previous studies, combining a hydrogen-rich polymer with boron carbide provides effective radiation shielding against both thermal and fast neutrons. Fast neutrons lose energy through elastic scattering with hydrogen and are then absorbed by boron [46]. In this study, as the filler content increased from 0.5 wt.% to 5 wt.%, the nano-B_4C composites showed improvements in neutron attenuation of up to 6.7%, 12.6%, 18.3%, and 24.4% for sample thicknesses of 2.5, 5, 7.5, and 10 mm, respectively. For the micro-B_4C composites, the corresponding improvements in neutron attenuation were 2.2%, 4.1%, 6.0%, and 8.0% for the same thicknesses. These findings are consistent with the results reported by Kaewsrithong *et al.*, who studied the thermal neutron shielding properties of unsaturated polyester resin reinforced with B_4C (0-20 wt.%). They found that increasing the B_4C content enhanced the total cross-section and reduced the HVL, with 20 wt.% B_4C composites showing the best performance. Consequently, both neutron absorption and shielding effectiveness improved [47].

In this study, the total neutron rate decreased more steeply with nano-B_4C fillers than with micro-B_4C fillers. As the sample thickness increased, the nano-B_4C composites demonstrated superior attenuation of 4.7%, 9.7%, 15%, and 20% compared to the micro-B_4C composites at thicknesses of 2.5, 5, 7.5, and 10 mm, respectively. Notably, the total neutron macroscopic cross-section in the polyester composites containing 1 wt.% nano-B_4C filler was slightly higher than that in composites with 2 wt.% micro-B_4C filler at the same thickness, as shown in table 1. Furthermore, the composite sample with 2 wt.% nano-B_4C filler exhibited a higher total neutron cross-section than the sample with 5 wt.% micro-B_4C filler. This indicates that the neutron absorption capability of the 2 wt.% nano-B_4C composites exceeds that of the 5 wt.% micro-B_4C composites.

The likelihood of neutron radiative capture depends significantly on the size and distribution of the B_4C particles within the composite. Due to their substantial interfacial area, nanoscale B_4C/polyester composites often demonstrate better performance than those using micron-scale fillers. This observation is consistent with published data. To develop polymer materials as lightweight, flexible, and easily processed shields for neutron radiation protection, incorporating nanofillers is essential [48]. According to the literature, neutron shielding efficiency and physical properties are both enhanced when nano-fillers are used instead of micro-fillers [49-51]. In conclusion, incorporating boron carbide nanoparticles into polyester composites significantly enhances their neutron attenuation capability compared to microparticles. This improvement is largely attributed to the more uniform particle distribution and higher surface interaction rates [52]. Thus, nano-sized B_4C particles improve neutron attenuation by providing higher reactivity and better dispersion [53, 54].

According to the simulation results, the particle size of the radiation shielding material plays an important role in shielding efficiency. Decreasing the particle size of the shielding material at each filler loading level resulted in improved radiation shielding properties. It appears that reducing the particle size and ensuring a homogeneous distribution of nano-B_4C particles increases the probability of collisions between incident thermal neutrons and the shielding material, thereby enhancing neutron attenuation [52].

Another study explored various materials for nano-shields, including boron compounds (B_4C) and ferric compounds in silicone resin, to reduce fast neutron exposure from an Am-Be neutron source. They reported macroscopic cross-sections ranging from 0.15 to 0.32 cm^{-1} for B_4C at 30-50% nanoparticle concentrations for a 2 cm thick sample [55]. According to the literature, for each thickness between 2.5 mm and 10 mm, macroscopic cross-sections for B_4C at 0.5-5% nanoparticle concentrations were approximately 0.15 to 0.43 cm^{-1}. Despite differences in filler percentage, sample thickness, and irradiation source, the macroscopic cross-sections are quite similar, indicating good agreement between the studies. It can also be noted that B_4C combined with unsaturated polyester resin (UPS) at lower thicknesses demonstrated better macroscopic cross-sections.

Due to limitations in producing samples with higher weight percentages of filler and greater thicknesses, our study may not fully capture the potential neutron attenuation performance of these composites. However, it does highlight the importance of incorporating B_4C particle fillers and comparing the performance of nano- and micro-sized fillers. From this, we can conclude that shielding efficacy depends on several factors, including the neutron energy spectrum, the mass fraction of B_4C, particle size, and dispersion.

CONCLUSION

The present study introduces a novel composite material designed for neutron radiation protection, comprising a polyester matrix reinforced with boron carbide (B_4C) in both nano- and micro-sized forms. Both experimental and simulation results confirm that these composites effectively attenuate neutrons emitted from a ^{239}Pu-Be source. Samples with greater

thicknesses and higher weight percentages of either micro- or nano-B_4C fillers demonstrate enhanced neutron attenuation. Furthermore, polyester composites containing nano-B_4C fillers exhibit superior attenuation properties compared to those reinforced with micro-B_4C fillers. This is attributed to their increased surface-to-volume ratio and improved dispersion within the matrix. Overall, these findings validate the suitability of nano-B_4C composites for high-efficiency radiation shielding applications.

Acknowledgments: The authors express their gratitude to all the individuals who took part in the study.
Funding: No funding.
Conflicts of interest: The authors declare that there is no conflict of interest.
Ethics approval: N/A
Consent to publish: Not applicable.
Author contribution: All authors contributed equally to the design, data collection, analysis, interpretation of data and the writing of the manuscript. All authors read and approved the final manuscript.
Using Artificial Intelligence Chatbots: We utilized AI-powered tools to check grammar and enhance the academic quality of the text, which was primarily written by the authors.

REFERENCES

1. Mustonen R, Bouvier G, Wolber G, *et al.* (1999) A comparison of gamma and neutron irradiation on Raji cells: effects on DNA damage, repair, cell cycle distribution and lethality. *Mutation Research,* ***429****(2): 169-75*.
2. Stewart RD, Streitmatter SW, Argento DC, *et al.* (2015) Rapid MCNP simulation of DNA double strand break (DSB) relative biological effectiveness (RBE) for photons, neutrons, and light ions. *Physics in Medicine and Biology,* ***60****(21): 8249-74*.
3. Akashi M, Hirama T, Tanosaki S, *et al.* (2001) Initial symptoms of acute radiation syndrome in the JCO criticality accident in Tokaimura. *Journal of Radiation Research,* ***42*** *(Suppl): S157-S66*.
4. Acharya MM, Baulch JE, Klein PM, *et al.* (2019) New concerns for neurocognitive function during deep space exposures to chronic, low dose-rate, neutron radiation. *eNeuro,* ***6****(4): ENEURO.0094-19.2019*.
5. Norbury JW, Slaba TC, Aghara S, *et al.* (2019) Advances in space radiation physics and transport at NASA. *Life Sciences in Space Research,* ***22****: 98-124*.
6. Piotrowski T (2021) Neutron shielding evaluation of concretes and mortars: a review. *Construction and Building Materials,* ***277****: 122238*.
7. Abdulrahman ST, Ahmad Z, Thomas S, *et al.* (2020) Introduction to neutron-shielding materials. Micro and nanostructured composite materials for neutron shielding applications: Woodhead Publishing, p: 1-23.
8. Kharita MH, Yousef S, AlNassar M (2011) Review on the addition of boron compounds to radiation shielding concrete. *Progress in Nuclear Energy,* ***53****(2): 207-11*.
9. Baxter L, Herrman K, Panthi R, *et al.* (2020) Thermoplastic micro- and nanocomposites for neutron shielding. Micro and nanostructured composite materials for neutron shielding applications: Woodhead Publishing, p: 53-82.
10. Mortazavi SMJ, Bevelacqua JJ, Rafiepour P, *et al.* (2024) Lead-free, multilayered, and nanosized radiation shields in medical applications, industrial, and space research. Advanced Radiation Shielding Materials: Elsevier, p. 305-22.
11. Sukegawa AM, Okuno K, Sakurai S (2009) High-heat-resistant neutron shielding resin. *Nuclear Technology,* ***168****(2): 553-8*.
12. El-Sarraf MA, El-Sayed Abdo A (2013) Insulating epoxy/barite and polyester/barite composites for radiation attenuation. *Applied Radiation and Isotopes,* ***79****: 18-24*.
13. Kandelbauer A, Tondi G, Zaske OC, *et al.* (2022) Unsaturated polyesters and vinyl esters. Handbook of Thermoset Plastics: William Andrew Publishing, p: 97-158.
14. Tuna T, Eker AA, Kam E (2021) Neutron shielding characteristics of polymer composites with boron carbide. *Journal of the Korean Physical Society,* ***78****: 566-73*.
15. Kaewsrithong K, Suriwong T, Julphunthong P, *et al.* (2023) Development and evaluation of boron carbide-modified unsaturated polyester resin for use as neutron radiation Protection. Journal of Physics: Conference Series, IOP Publishing.
16. Uddin Z, Yasin T, Shafiq M, *et al.* (2020) On the physical, chemical, and neutron shielding properties of polyethylene/boron carbide composites. *Radiation Physics and Chemistry,* ***166****: 108450*.
17. Oğul H, Polat H, Akman F, *et al.* (2022) Gamma and neutron shielding parameters of polyester-based composites reinforced with boron and tin nanopowders. *Radiation Physics and Chemistry,* ***201****: 110474*.
18. Park J, Her S, Cho S, Woo SM, Bae S (2022) Synthesis and characterization of Polyethylene/B4C composite, and its neutron shielding performance in cementitious materials: Experimental and simulation studies. *Cement and Concrete Composites,* ***129****: 104458*.
19. Wang W, Li Q, Li Q, Yang X, Le G (2022) A review of irradiation stability of lithium hydride neutron shielding material. *Materials Science and Technology,* ***32****(5): 434-7*.
20. Schuy C, Tessa C, Horst F, *et al.* (2022) Experimental assessment of lithium hydride's space radiation shielding performance and Monte Carlo benchmarking. *Radiation Research,* ***191****(2): 154-61*.
21. El-Khatib AM, Hamada MS, Alabsy MT, *et al.* (2021) Fast and thermal neutrons attenuation through micro-sized and nano-sized CdO reinforced HDPE composites. *Radiation Physics and Chemistry,* ***180****: 109245*.
22. Moradgholi J and Mortazavi SMJ (2021) Developing a radiation shield and investigating the mechanical properties of polyethylene-polyester/CdO bilayer composite. *Ceramics International,* ***48****(4): 5246-51*.
23. Babu NK, Muthukumaran S, Arokiasamy S, *et al.* (2018) Thermal and mechanical behavior of the coir powder filled polyester micro-composites. *Journal of Natural Fibers,* ***17****(7): 1058-1068*.
24. Brown DA, Chadwick MB, Capote R, *et al.* (2018) ENDF/B-VIII.0: The 8th major release of the nuclear reaction data library with CIELO-project cross sections, New standards and thermal scattering data. *Nuclear Data Sheets,* ***148****: 1-142*.
25. Li X, Wu J, Tang C, He Z, Yuan P, Sun Y, *et al.* (2019) High temperature resistant polyimide/boron carbide composites for neutron radiation shielding. *Composites Part B: Engineering,* ***159****: 355-61*.
26. Tamayo P, Thomas C, Rico J, *et al.* (2020) Review on neutron-absorbing fillers. Micro and nanostructured composite materials for neutron shielding applications: Woodhead Publishing, p: 25-52.
27. Harrison C, Weaver S, Bertelsen C, *et al.* (2008) Polyethylene/boron nitride composites for space radiation shielding. *Journal of Applied Polymer Science,* ***109****(4): 2529-38*.
28. Shin JW, Lee JW, Yu S, *et al.* (2014) Polyethylene/boron-containing composites for radiation shielding. *Thermochimica Acta,* ***585****: 5-9*.
29. Adeli R, Shirmardi S, Bagheri R (2017) Theory and simulation investigation of low-energy neutron shielding for different boron compounds. *Journal of Testing and Evaluation,* ***45****(5): 1570-6*.
30. Özdemir T, Güngör A, Reyhancan İA (2017) Flexible neutron shielding composite material of EPDM rubber with boron trioxide: Mechanical, thermal investigations and neutron shielding tests. *Radiation Physics and Chemistry,* ***131****: 7-12*.
31. Chkhartishvili L, Makatsaria S, Gogolidze N, *et al.* (2023) Obtaining boron carbide and nitride matrix nanocomposites for neutron-shielding and therapy applications. *Condensed Matter,* ***8****(4): 92.*
32. Dong M, Zhou S, Xue X, *et al.* (2021) The potential use of boron containing resources for protection against nuclear radiation. *Radiation Physics and Chemistry,* ***188****: 109601*.
33. Kipcak AS, Gurses P, Derun EM, *et al.* (2013) Characterization of boron carbide particles and its shielding behavior against neutron radiation. *Energy Conversion and Management,* ***72****: 39-44*.
34. Castley D, Goodwin C, Liu J (2019) Computational and experimental comparison of boron carbide, gadolinium oxide, samarium oxide, and graphene platelets as additives for a neutron shield. *Radiation Physics and Chemistry,* ***165****: 108435*.

35. Swinhoe, M. T., Hutchinson, J. D., & Rinard, P. M. (2024). Neutron interactions with matter. In Nondestructive assay of nuclear materials for safeguards and security. *Cham: Springer Nature Switzerland. p. 307-323*.
36. Orak S, Yılmaz Baysoy D (2013) Neutron shielding properties of concrete with boron and boron containing mineral. *Academic Platform Journal of Engineering and Science, **1**: 15-9*.
37. Biswas R, Sahadath H, Mollah AS, Huq MF (2016) Calculation of gamma-ray attenuation parameters for locally developed shielding material: Polyboron. *Journal of Radiation Research and Applied Sciences, **9**(1): 26-34*.
38. Fåk B, Rols S, Manzin G, *et al.* (2022) Panther-the new thermal neutron time-of-flight spectrometer at the ILL. EPJ Web of Conferences, EDP Sciences.
39. Agostinelli S, Allison J, Amako KA, *et al.* (2003) GEANT4 - a simulation toolkit. *Nuclear Instruments and Methods in Physics Research Section A: Accelerators, Spectrometers, Detectors and Associated Equipment, **506**(3): 250-303*.
40. Lei F, Truscott RR, Dyer CS, *et al.* (2002) MULASSIS: A Geant4-based multilayered shielding simulation tool. *IEEE Transactions on Nuclear Science, **49**(6): 2788-93*.
41. Alabsy MT and Elzaher MA (2023) Radiation shielding performance of metal oxides/EPDM rubber composites using Geant4 simulation and computational study. *Scientific Reports, **13**(1): 7744*.
42. Alzahrani, J. S., Alrowaili, Z. A., Alqahtani, M. S., Adam, M., Olarinoye, I. O., & Al-Buriahi, M. S. (2023). Neutron attenuation features and elastic properties of silicate glasses containing Ta2O5, and Li2O. *Applied Radiation and Isotopes, **199**: 110896*.
43. More CV, Akman F, Dilsiz K, *et al.* (2023) Estimation of neutron and gamma-ray attenuation characteristics of some ferrites: Geant4, FLUKA and WinXCom studies. *Applied Radiation and Isotopes, **197**: 110803*.
44. Jamil M, Rhee JT, Jeon YJ (2013) Simulation response of B4C-coated PPAC for thermal neutrons using GEANT4 Monte Carlo approach. *Nuclear Instruments and Methods in Physics Research Section A: Accelerators, Spectrometers, Detectors and Associated Equipment, **718**: 240-2*.
45. Chen Z, Yang P, Lei Q, *et al.* (2019) Comparison of BNCT dosimetry calculations using different GEANT4 physics lists. *Radiation Protection Dosimetry, **187**(1): 88-97*.
46. Tcherdyntsev VV, Kaloshkin SD, Lunkova AA, *et al.* (2014) Structure, mechanical and tribological properties of radiation cross -linked ultrahigh molecular weight polyethylene and composite materials based on it. *Journal of Alloys and Compounds, **586**: S443-S5*.
47. Kaewsrithong K, Suriwong T, Julphunthong P, *et al.* (2023) Development and evaluation of boron carbide-modified unsaturated polyester resin for use as neutron radiation Protection. *Journal of Physics: Conference Series, **2653**(1): 012065.*
48. More CV, Alsayed Z, Badawi MS, *et al.* (2021) Polymeric composite materials for radiation shielding: a review. *Environmental Chemistry Letters, **19**(3): 2057-90*.
49. Kim J, Lee BC, Uhm YR, Miller WH (2014) Enhancement of thermal neutron attenuation of nano-B4C, -BN dispersed neutron shielding polymer nanocomposites. *Journal of Nuclear Materials, **453**(1-3): 48-53*.
50. Mesbahi A, Verdipoor K, Zolfagharpour F, *et al.* (2019) Investigation of fast neutron shielding properties of new polyurethane-based composites loaded with BC, BeO, WO, ZnO, and GdO micro-and nanoparticles. P*olish Journal of Medical Physics and Engineering, 25(4): 211-9*.
51. Mokhtari K, Saadi MK, Panahi HA, *et al.* (2021) The shielding properties of the ordinary concrete reinforced with innovative nano polymer particles containing PbO–H3BO3 for dual protection against gamma and neutron radiations. *Radiation Physics and Chemistry, **189**: 109711*.
52. Soltani Z, Beigzadeh A, Ziaie F, *et al.* (2016) Effect of particle size and percentages of Boron carbide on the thermal neutron radiation shielding properties of HDPE/B4C composite: Experimental and simulation studies. *Radiation Physics and Chemistry, **127**: 182-7*.
53. Vegari A, Abdisaray A, Mostafanejad K, *et al.* (2024) High-density polyethylene (HDPE)-incorporated boron carbide and boric acid nanoparticles as a nanoshield of photoneutrons from medical linear accelerators. *International Journal of Radiation Biology, **100**: 1-10*.
54. Ozdogan H, Kacal MR, Kilicoglu O, *et al.* (2025) Experimental, simulation, and theoretical investigations of gamma and neutron shielding characteristics for reinforced with boron carbide and titanium oxide composites. *Radiation Physics and Chemistry, **226**: 112167*.
55. Afkham Y, Mesbahi A, Alemi A, *et al.* (2020) Design and fabrication of a Nano-based neutron shield for fast neutrons from medical linear accelerators in radiation therapy. *Radiation Oncology, **15**(1): 105.*